Available online at www.sciencedirect.com
SCIENCE DIRECT
Carbohydrate Polymers 65 (2006) 235–242
Carbohydrate Polymers
www.elsevier.com/locate/carbpol

# The adsorption of globular proteins, bovine serum albumin and β-lactoglobulin, on poly-L-lysine–furcellaran multilayers

K. Laos [1], R. Parker, J. Moffat, N. Wellner, S.G. Ring *

*Institute of Food Research, Norwich Research Park, Colney, Norwich NR4 7UA, UK*

Received 18 November 2005; accepted 9 January 2006
Available online 24 February 2006

**Abstract**

The formation of multilayer films of poly-L-lysine (PLL) and furcellaran was investigated using surface plasmon resonance (SPR), quartz crystal microbalance with dissipation monitoring (QCM-D) and Fourier transform infrared spectroscopy with attenuated total reflection (FTIR-ATR). The progressive form of the growth of mass of polymer deposited for the multilayer was consistent with the ability of the PLL to diffuse within the furcellaran layer. Using the same experimental approaches, the pH-dependent adsorption of the globular proteins, bovine serum albumin (BSA) and β-lactoglobulin (BLG), to the PLL–furcellaran multilayers was also examined. Substantial adsorption was observed even at pH's above the isoelectric point where the net charge on the protein was of the same sign as that of the furcellaran.


*Keywords:* Furcellaran; Bovine serum albumin; β-Lactoglobulin; Multilayer

## 1. Introduction

Polyelectrolyte multilayers may be formed by the sequential dipping of a charged surface into solutions of a polyanion and polycation (Decher, 1997). A requirement for multilayer formation is that the binding of polyelectrolyte to the growing multilayer surface results in charge reversal, permitting the subsequent deposition of oppositely charged polyelectrolyte. Polyelectrolyte multilayers are non-equilibrium structures whose properties are strongly influenced by the conditions of their preparation, including molecular size (Picart et al., 2002; Sui, Salloum, & Schlenoff, 2003); ionic strength (Dubas & Schlenoff, 2001; Schlenoff, Ly, & Li, 1998) and for weak polyelectrolytes, pH (Burke & Barrett, 2003; Shiratori & Rubner, 2000).

The interaction between opposite charges may also be used to incorporate other species/structures into the growing multilayer such as protein polyampholytes (Caruso, Furlong, Ariga, Ichinose, & Kunitake, 1998; Gergely et al., 2004; Ladam et al., 2000; Salloum & Schlenoff, 2004); unilamellar vesicles (Michel, Vautier, Voegel, Schaaf, & Ball, 2004); and wax droplets (Glinel et al., 2004). This versatility means that these structures have a potentially wide range of application as barriers and coatings (Quinn & Caruso, 2004; Shi & Caruso, 2001). Most studies have been performed with synthetic polyelectrolytes. For some applications, including those in the food and pharmaceutical sectors, it is important to consider the fabrication of biopolymer multilayers. Recent examples include alginate–poly-L-lysine (Elbert, Herbert, & Hubbell, 1999); hyaluronan–poly-L-lysine (Burke & Barrett, 2003); hyaluronan–chitosan (Richert et al., 2004); and pectin–chitosan (Marudova, Lang, Brownsey, & Ring, 2005).

In this article, we examine the fabrication of a furcellaran/poly-L-lysine multilayer using surface plasmon resonance (SPR), FTIR-ATR and a quartz crystal microbalance with dissipation monitoring (QCM-D). Furcellaran is a sulphated galactan, and therefore a strong polyelectrolyte, which can be extracted from the seaweed *Furcellaria lumbricalis*

* Corresponding author.
*E-mail address:* steve.ring@bbsrc.ac.uk (S.G. Ring).
[1] Present address: Department of Food Processing, Tallinn University of Technology, Ehitajate tee 5, 19086 Tallinn, Estonia. Tel.: +01603 255000.

0144-8617/$ - see front matter © 2006 Elsevier Ltd. All rights reserved.
doi:10.1016/j.carbpol.2006.01.010

(Lahaye, 2001; Truus, Vaher, Usov, Pehk, & Kollist, 1997). It consists of residues of (1 → 3) β-D-galactopyranose and its 4-sulphate and (1 → 4) α-D-galactopyranose. The latter may exist as a 3,6-anhydro residue which may be partially sulphated at position 2. Structurally, furcellaran is related to the algal polysaccharide κ-carrageenan, with a major structural difference being that furcellaran has a smaller degree of sulphation (Truus et al., 1997). We also investigate the capacity of the multilayer to adsorb globular proteins, including bovine serum albumin and β-lactoglobulin.

## 2. Materials and methods

### 2.1. Materials

Furcellaran was obtained from FMC Food Ingredients. The $Na^+$ furcellaran was obtained by elution through an ion-exchange (Amberlite IR-120) column in the $Na^+$ form at 4 °C. The intrinsic viscosity of 492 mL $g^{-1}$ indicates a relatively large molecular size in 0.1 M NaCl. Poly-L-lysine hydrobromide (PLL) with a mean degree of polymerisation of 70, bovine serum albumin (BSA) and β-lactoglobulin (BLG) were obtained from Sigma–Aldrich, UK. For multilayer fabrication, aqueous biopolymer solutions (0.6 mg $mL^{-1}$) were prepared in 0.1 M, pH 5.6, acetate buffer containing 0.03 M NaCl. For the protein binding studies, aqueous protein solutions (0.6 mg $mL^{-1}$), in 0.01 M acetate or phosphate buffer with pH's in the range 5.0–8.0 containing 0.03 M NaCl, were used.

### 2.2. Surface plasmon resonance

Measurements were carried out using a Biacore X instrument. The sensing element was a thin film of gold (~50 nm), deposited on a glass substrate mounted in a sensor chip cartridge (Biacore AB, Uppsala, Sweden). The instrument monitors changes in refractive index adjacent to the surface of the gold film by measuring the intensity of polarised light reflected from the reverse side of the glass–gold interface. The plasmon resonance causes a minimum in intensity to occur at a certain angle of incidence, $\theta_m$. The value of $\theta_m$ varies with changes in refractive index of the region adjacent the gold surface. The size of this region depends on the penetration of an evanescent wave into the flow channel which typically extends 25–50% of the wavelength of the incident light from the surface (Jung, Campbell, Chinowsky, Mar, & Yee, 1998). The Biacore instrument reports $\theta_m$ in resonance units (RU) where 10,000 RU represents a shift in $\theta_m$ of 1°. The instrument was calibrated at 20 °C with methanol–water and sucrose–water systems of known refractive indices. The response to changes in refractive index was found to be linear with a shift in $\theta_m$ of 86.6° per unit change in refractive index. The change in $\theta_m$, $\Delta\theta$, due to the adsorption of a uniform adsorbed layer is related to refractive index through the relationship (Jung et al., 1998):

$$\Delta\theta = m(n_{adl} - n_s)\left[1 - \exp(-2h/d_{spr})\right], \quad (1)$$

where $n_{adl}$ and $n_s$ are the refractive indices of the adsorbed layer and bulk solution, respectively. The thickness of the layer is $h$ and $d_{spr}$ is the characteristic decay length of the evanescent electromagnetic field, and can be estimated as $37 \pm 13\%$ of the wavelength of incident light (760 nm) (Jung et al., 1998). If it is assumed that the refractive index of the layer is proportional to the adsorbate concentration, the exponential in Eq. (1) can be expanded to yield an explicit expression for the mass of adsorbed polymer per unit area ($c_{spr}$)

$$c_{spr} = \frac{d_{spr} c_{max} \Delta\theta}{2m(n_{ads} - n_S)}, \quad (2)$$

where $c_{max}$ and $n_{ads}$ are the density and refractive index of the pure adsorbate. Expanding the exponential is accurate to within 10% when $h < 0.1 d_{spr}$.

Multilayers were built up by the layer-by-layer technique at a flow rate of 25 μL $min^{-1}$. A buffer baseline was established, then a PLL base layer was laid down by injecting 50 μL of PLL solution, followed by ~75 μL of buffer, 50 μL of furcellaran solution and a buffer rinse as before. The sequence was repeated to form the multilayer which was then ready for globular protein adsorption studies. Between each experiment the gold surface was regenerated by flowing 0.1 M NaOH through the measurement cell. All measurements were made at 20 °C.

### 2.3. FTIR-ATR spectroscopy

FTIR has been extensively used to probe polyelectrolyte adsorption at surfaces (Sukhishvili, Dhinojwala, & Granick, 1999; Sukhishvili & Granick, 1999). Infrared spectra were collected on a Nicolet 860 FTIR (Thermo Nicolet) spectrometer fitted with a micro CIRCLE liquid ATR cell (Spectra-Tech, Warrington, UK). The ATR crystal was a cylindrical ZnSe prism, with 11 internal reflections, mounted in a thermostatted steel jacket set at a temperature of 20 °C. Biopolymer solutions were prepared as described above using $D_2O$ instead of $H_2O$. One millilitre of biopolymer solution was injected and left for 16 min. After each deposition step the cell was rinsed with 2 mL of deuterated buffer. Spectra were accumulated by averaging 1024 scans at a resolution of 2 $cm^{-1}$ and subtracted from a background of the buffer alone.

In the ATR mode, a light beam strikes the interface between a medium of high refractive index ($n_1$) and a medium of low refractive index ($n_2$). The beam is totally reflected if the angle of incidence $\theta_i$ is larger than the critical angle $\theta_c$, where $\theta_c = \sin^{-1}(n_2/n_1)$. At the point of reflection an evanescent wave of exponentially decreasing intensity penetrates the medium of lower refractive index. The depth of penetration ($d_{ir}$) of the evanescent wave – defined as the distance normal to the interface at which the intensity falls to $1/e$ of the intensity at the surface – is given by:

$$d_{ir} = \frac{\lambda}{2\pi n_1 (\sin^2\theta_i - n_{12}^2)^{1/2}}, \quad (3)$$

where $\lambda$ is the wavelength of the light in vacuum and $n_{12} = n_2/n_1$. The refractive index of the crystal is 2.41 and that of the dilute polymer in solution is 1.33. The angle of incidence is 45°. As the penetration depth is large (~631 nm at 1645 $cm^{-1}$) compared to the layer thickness, the FTIR signal potentially contains contributions from the polymer in bulk solution as well as from the polymer adsorbed onto the surface of the crystal. However, at the concentrations used in the present experiment, the polymer in solution does not make a significant contribution to the observed spectra.

### 2.4. Quartz crystal microbalance

Measurements were carried out using a D300 quartz crystal microbalance with dissipation monitoring (QCM-D) from Q-Sense AB (Västra Frölunda, Sweden) with a QAFC 302 axial flow measurement chamber. The sensing element is a disc-shaped, AT-cut piezoelectric quartz crystal sandwiched between two gold electrodes. The crystal is excited to oscillation at its fundamental resonant frequency (~5 MHz). A small mass deposited ($\Delta m$) on the gold sensing surface will cause a decrease in resonant frequency ($\Delta f$). If the mass is deposited evenly and is sufficiently rigid then the mass adsorbed is directly proportional to the change in frequency according to the Sauerbrey equation (Sauerbrey, 1959):

$$\Delta m = -C\Delta f/n, \quad (4)$$

where $C$ is the mass sensitivity constant ($C = 17.7\ ng\ cm^{-2}\ Hz^{-1}$ for a 5 MHz crystal (Hook, 1997)) and $n$ is the overtone number ($n = 1, 3, 5, \ldots$). For elastic, cross-linked gel networks, the mass of solvent trapped within the gel contributes to the overall mass adsorbed and the observed frequency change. For viscoelastic materials the adsorbed mass does not fully couple to the oscillation of the crystal and hence dampens the oscillation. The QCMD measures this dissipation from the response of the crystal at its resonant frequency (5 MHz) and at three of its overtones (15, 25 or 35 MHz) following the excitation of the crystal to resonance. The decrease in the amplitude of the oscillation with time provides a single-exponential decay constant which characterises the dissipation.

The QCMD response to dissipative viscoelastic films has been modelled using a Voigt model (Voinova, Rodahl, Jonson, & Kasemo, 1999). The full expression for the resonance frequency and dissipation shifts with a thick adsorbed layers can be concisely expressed using complex variables. Some physical insight into how the material properties of the bulk liquid and adsorbed layer affect the QCMD response can be obtained for single thin viscoelastic adsorbed layers for which the equations simplify as follows (retaining Voinova et al.'s notation):

$$\Delta f \approx -\frac{1}{2\pi\rho_0 h_0}\left\{\frac{\eta_3}{\delta_3} + h_1\rho_1\omega - 2h_1\left(\frac{\eta_3}{\delta_3}\right)^2 \frac{\eta_1\omega^2}{\mu_1^2 + \omega^2\eta_1^2}\right\}, \quad (5)$$

$$\Delta D \approx \frac{1}{\pi f \rho_0 h_0}\left\{\frac{\eta_3}{\delta_3} + 2h_1\left(\frac{\eta_3}{\delta_3}\right)^2 \frac{\mu_1\omega}{\mu_1^2 + \omega^2\eta_1^2}\right\}, \quad (6)$$

where $\rho_0$ and $h_0$ are the density and thickness of the crystal, respectively. The viscosity of the bulk liquid is $\eta_3$, and $\delta_3$ ($=(2\eta_3/\rho_3\omega)^{1/2}$) is the viscous penetration depth of the shear wave in the bulk liquid and $\rho_3$ is the liquid's density. The thickness, density, viscosity and elastic shear modulus of the adsorbed layer are represented by $h_1$, $\rho_1$, $\eta_1$ and $\mu_1$, respectively; $\omega$ is the angular frequency of the oscillation. The first term in the brackets in Eqs. (5) and (6), $\eta_3/\delta_3$, is the frequency and dissipation shift due to immersing the crystal oscillator in the bulk liquid, a factor which is effectively constant in our experiments. The second term in the brackets in Eq. (5) is the Sauerbrey term, as in Eq. (4), due to the hydrated mass of the adsorbed layer. As this term is proportional to frequency it is common to present the frequency shift as $\Delta f/n$ to take this into account. The final term in the brackets in Eq. (5) and (6) arises due to viscoelasticity. In Eq. (5) this term is negative so that viscoelasticity reduces the frequency shift and the use of the Sauerbrey equation would underestimate the mass adsorbed and hydrated layer thickness. Modelling software (QTools) supplied with the QCMD use the full thick layer expressions to model the response. The program finds a best fit using a Simplex algorithm to find the minimum in the sum of the squares of the scaled errors between the experimental and model $\Delta f$ and $\Delta D$ values. By assuming the density and viscosity of the bulk liquid ($\rho_3$ and $\eta_3$) are 1000 $kg\ m^{-3}$ and 1.0 mPa s, respectively, and a fixed density of the layer ($\rho_1$), the package estimates the viscosity, shear modulus and the thickness of the adsorbed layer.

The formation of multilayers was investigated at 20 °C. Starting with the system primed with buffer solution, a base layer is formed by first flowing ~2.0 mL of PLL solution into a thermostatic coil in the measurement head to flush out the previous solution and allow the solution to reach thermal equilibrium. After 5 min, ~0.5 mL of this solution was allowed to flow into the measurement cell to replace the existing solution, driven by the head of liquid in the sample reservoir which flows into the thermostatic coil. The same procedure was repeated with buffer, followed by biopolymer solution, buffer solution, and so on. Between each experiment the crystal chip was cleaned by sonication in 99% ethanol solution for 5 min followed by sonication in 2% Hellmanex solution (Hellma UK Ltd.) for 5 min. The chips were rinsed in distilled water and then dried with $N_2$.

## 3. Results and discussion

### 3.1. Multilayer fabrication – SPR

PLL–furcellaran multilayers were prepared by layer-by-layer deposition at pH 5.6. Under these conditions both PLL and furcellaran are essentially fully charged. PLL

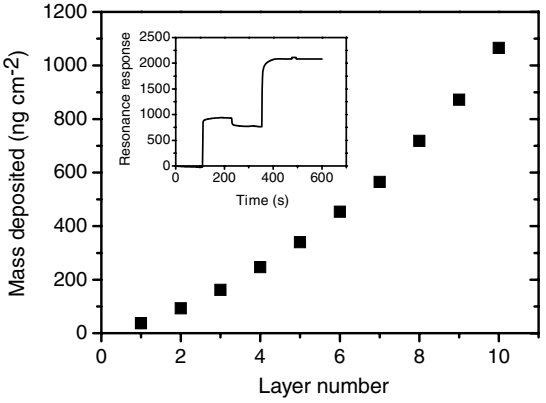


Fig. 1. Mass of polymer deposited as a function of layer number for the buildup of a PLL–furcellaran multilayer. Inset shows SPR response as a function of time for the deposition of the fifth and sixth layers.

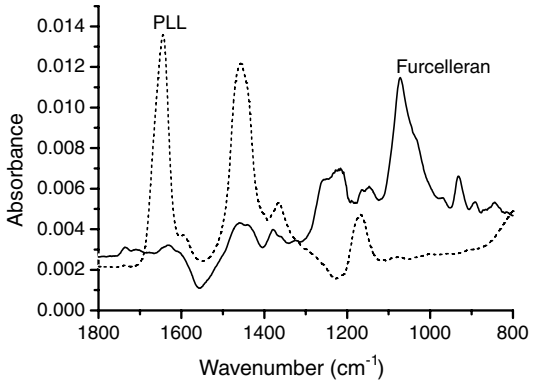


Fig. 2. Solution FTIR-ATR spectra of PLL and furcellaran in $D_2O$ in the region 1800–800 $cm^{-1}$.

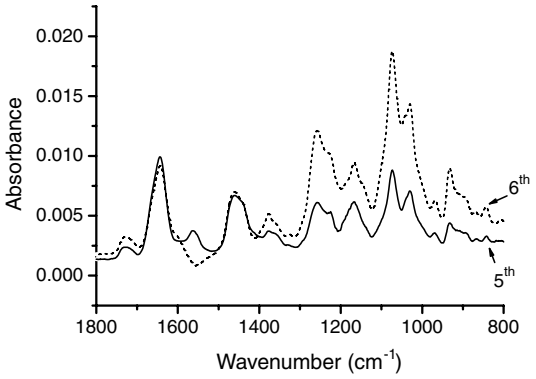


Fig. 3. FTIR-ATR spectra of PLL–furcellaran multilayer in $D_2O$ in the region 800–1800 $cm^{-1}$ after deposition of the fifth (PLL) and sixth (furcellaran) layers.

was initially deposited on a gold surface followed by attachment of furcellaran. Through the sequential deposition of PLL and furcellaran, a 10-layer multilayer was fabricated. The build up of the multilayer was followed by surface plasmon resonance. In Fig. 1 is shown the mass deposited as a function of layer number. The mass deposited shows a relatively smooth progressive increase with each new layer, with approximately equal amounts of PLL and furcellaran being laid down. The inset in Fig. 1 shows a detail of the surface plasmon resonance response for the deposition of the fifth (PLL) and sixth layers (furcellaran). The deposition of PLL results in a step change in response with a limited solubilisation following the buffer rinse. The progressive increase with increasing layer number is characteristic of polyelectrolyte multilayers in which one, lower molecular size component, has the ability to diffuse to the growing multilayer surface resulting in an increased capture of the next layer of oppositely charged polymer (Lavalle, Picart, et al., 2004; Lavalle & Vivet et al., 2004; Picart et al., 2002). Furcellaran carries less charge per unit mass than poly-L-lysine, because of its higher average molecular mass per repeating unit, and through one residue in every ~2.8 being charged. A consequence of the approximately equal mass deposition of furcellaran and PLL, assuming that both species are fully charged, is that the multilayer carries an excess of positive charge.

### 3.2. Multilayer fabrication – FTIR-ATR

FTIR-ATR was used to obtain information on the chemical characteristics of the deposited species. Fig. 2 compares solution spectra of furcellaran and PLL at concentrations of 0.3% and 0.8% w/w at pD 5.6. The PLL spectrum has strong absorbances at 1643 and 1460 $cm^{-1}$. The latter is the amide II′ band which includes contributions from CN stretching and other backbone modes. The absorbance at 1643 $cm^{-1}$ is the amide I band, the precise location of which is conformation dependent, and for PLL in a random coil conformation (Jackson, Haris, & Chapman, 1989) occurs in the range 1643–1648 $cm^{-1}$. The furcellaran spectrum is similar to reported spectra of κ-carrageenan and includes features which have been assigned to 3,6-anhydro-D-galactose (932 $cm^{-1}$) and glycosidic linkages (1075 $cm^{-1}$) (Pereira, Sousa, Coelho, Amado, & Ribeiro-Claro, 2003; Volery, Besson, & Schaffer-Lequart, 2004). The spectra of assembled PLL–furcellaran multilayer films in the region 800–1800 $cm^{-1}$ are shown in Fig. 3. The spectra shown are those obtained after the deposition of the third PLL layer (layer 5) and the third furcellaran layer (layer 6). The bands at 1456 and 1643 $cm^{-1}$ are characteristic of the presence of PLL in the multilayer. The subsequent addition of furcellaran causes little change in the peak absorbance of these bands but does lead to an increase in absorbance of the bands associated with furcellaran at 932 and 1075 $cm^{-1}$. The alternating, stepwise addition is shown by examining how the absorbance of bands characteristic of furcellaran (1075 $cm^{-1}$) and PLL (1643 $cm^{-1}$) increases with increasing number of layers (Fig. 4).

### 3.3. Multilayer fabrication – QCM-D

The assembly of the multilayer film was monitored by QCM-D starting with a PLL layer (Fig. 5a). For clarity,

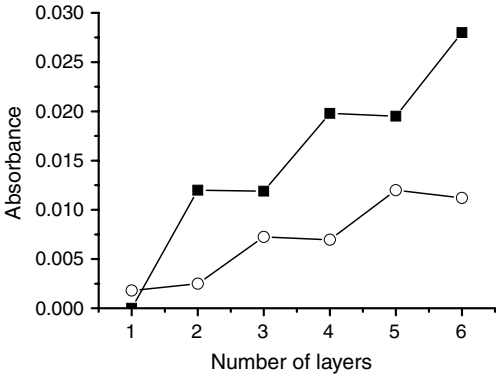


Fig. 4. The IR absorbance of PLL–furcellaran multilayer at 1075 (■) and 1643 $cm^{-1}$ (○) as a function of number of layers.

we report QCM-D data only for the third harmonic (15 MHz). Fig. 5a shows the frequency shift for the deposition of the first five layers starting with the deposition of PLL on the sensor surface. The decrease in $\Delta f$ observed for the first PLL and furcellaran layers is associated with an increase in adsorbed hydrated mass. Subsequent addition of PLL to the furcellaran layer leads to little significant change in $\Delta f$ (Figs. 5a and b). The trends observed for layer deposition using QCM-D are qualitatively different from those observed by SPR and FTIR-ATR, with the latter techniques probing the mass of polymer deposited and the QCM-D probing hydrated mass. The large response during the contact of the film with the polyanion solution and the very small response during contact with polycation solution (Figs. 5a and b) suggest that the smaller molecular size polycationic PLL is diffusing within the furcellaran layer, and that the observed QCM-D response is a balance between the small increase in mass associated with the deposition of PLL, and its effect on deswelling the multilayer arising as a result of the replacement of monovalent cationic counterions with a polyvalent counterion (PLL). The QCM-D experiment also contains information on the viscous dissipation of the multilayer (Fig. 5c). After deposition of the first furcellaran layer, addition of PLL decreases the dissipation indicating that PLL cross-links the furcellaran layer and, interpreting this change using the fit to the Voigt viscoelastic model, a reduction in hydrated mass and shrinkage of the adsorbed layer. This phenomenon has previously been observed in the assembly of high DE pectin–PLL multilayers (Krzeminski et al., 2006).

The hydrated mass from the QCM-D modelling, combined with polymer mass from the SPR, yields a solid concentration of $7.0 \pm 1.0\%$ w/w for the adsorbed layer, indicating that under these conditions of preparation a relatively hydrated, porous multilayer was formed.

### 3.4. Globular protein binding to the multilayer

Six-layer PLL–furcellaran multilayers were prepared with furcellaran as the topmost layer. The binding of the

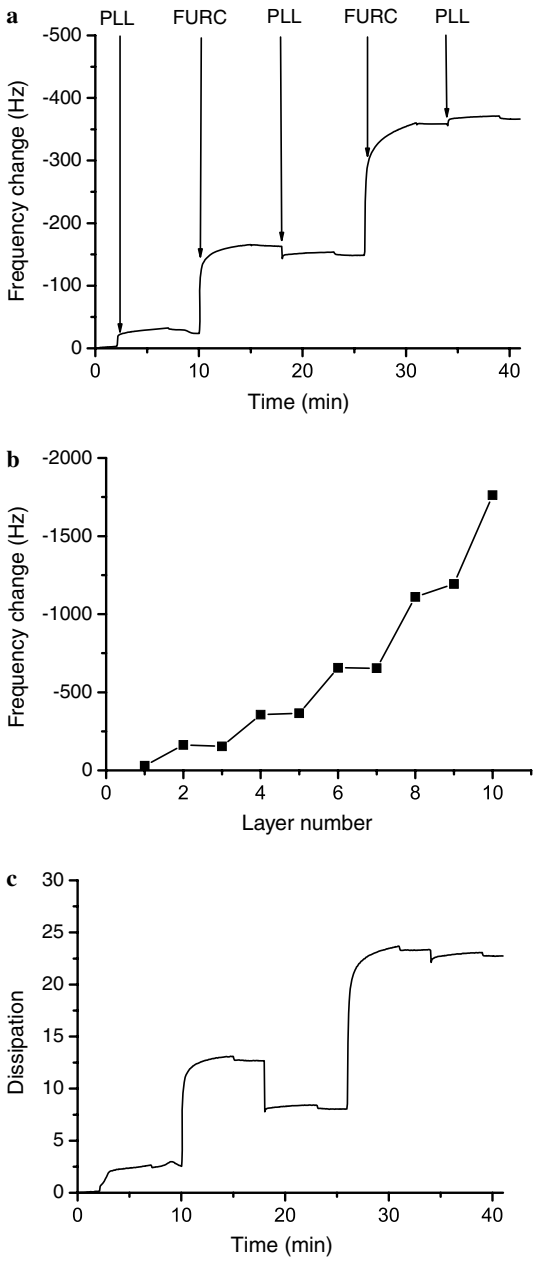


Fig. 5. (a) Plot of frequency change of QCM-D 15 MHz harmonic versus time for the assembly of the first five layers. (b) Plot of frequency change of QCM-D 15 MHz harmonic versus layer number for the assembly of a 10-layer multilayer. (c) Plot of QCM-D dissipation (15 MHz harmonic) versus time for the assembly of the first five layers.

globular proteins, BSA and BLG, to the multilayer was examined as a function of pH. Figs. 6a and b show the FTIR spectra of the multilayer before and after the binding of BSA and BLG at pH 5.0. There is a substantial spectral change on binding, with a particularly marked increase in the absorbance of the amide I and amide II′ bands. As the isoionic point of the isolated proteins is ~5.3 for defatted BSA (Tanford, Swanson, & Shore, 1955) and ~5.1 for BLG (Cannan, Palmer, & Kibrick, 1942) at pH 5.0, it is expected that the proteins will carry a small net positive charge. Solution studies on the interaction of globular

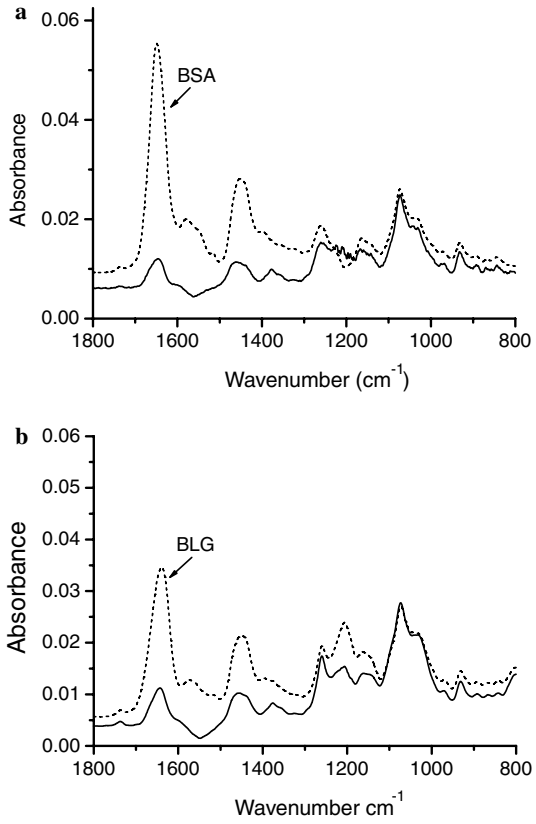


Fig. 6. (a) FTIR-ATR spectra of BSA deposition in $D_2O$ at pD 5.0 to third furcellaran layer (sixth layer). (b) FTIR spectra of BLG deposition in $D_2O$ at pD 5.0 to third furcellaran layer (sixth layer).

proteins with polyanions show that protein–polyelectrolyte complexes may be formed at pHs where the protein carries a net charge of the same sign as the polyelectrolyte (Hallberg & Dubin, 1998; Mattison, Dubin, & Brittain, 1998; Seyrek, Dubin, Tribet, & Gamble, 2003), with a more substantial aggregation or coacervation occurring below the isoelectric point when the protein acquires a net positive charge. In the region where both polymers carry a net charge of the same sign it is considered that the polyelectrolyte interacts with oppositely charged patches on the protein surface. The pH dependence of the adsorption of BSA and BLG to the PLL–furcellaran multilayer is shown in Fig. 7. Over the pH range 6.5–8 there is relatively little adsorption. As the pH is reduced to 5.0 there is a progressive increase in the amount adsorbed, and the observed behaviour is comparable to the generic complexation behaviour of polyelectrolytes and proteins which is observed in aqueous solution, and more particularly the observed complexation of furcellaran and globular proteins (Laos, Brownsey, & Ring, 2005). The pH-dependent adsorption was reversible. For both BSA and BLG the amount adsorbed at pH 5.0, calculated from the SPR resonance response, is ~650 ng $cm^{-2}$, substantially more than the amount of PLL that would be deposited on the furcellaran layer (cf. Fig. 1), and partially reflecting differences in mass/charge ratio. Over the pH range 6.5–5 the PLL–furcellaran multilayer shows a limited change in hydration leading to a frequency response in the QCMD experiment of $< -50$ Hz. The sign of the frequency response indicates that deposition of the globular proteins leads to an increase in hydrated mass, and the effect of partially neutralising the charge on the furcellaran with a polyampholyte (leading to deswelling, and mass loss) is more than compensated for by the mass of protein deposited. This is in contrast to the behaviour observed on PLL deposition and reflects differences in mass/charge ratio for the different species. The observed pH-dependent response (Fig. 7) is similar to the observed pH-dependent complexation of the globular proteins BSA and BLG with furcellaran (Laos et al., 2005).

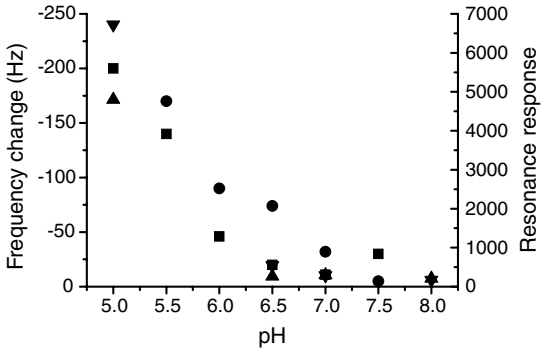


Fig. 7. Dependence of QCM-D frequency change (15 MHz harmonic), and SPR resonance response as a function of pH for the adsorption of BSA ▼ (SPR); ● (QCMD); and BLG ▲ (SPR); ■ (QCMD) on a 6-layer PLL–furcellaran multilayer.

Studies on the binding of globular proteins to polyelectrolyte multilayers show that the observed behaviour may be rather complex (Gergely et al., 2004; Ladam et al., 2000; Salloum & Schlenoff, 2004). There is general agreement that electrostatic interactions dominate the observed behaviour. In a recent study, it was found that the amount of protein adsorbed showed characteristically different behaviour depending on the charge on the terminating layer. It was proposed that the protein was drawn into the whole multilayer when the terminating layer was of opposite charge, whereas a more limited adsorption occurred when the terminating layer was of like charge (Salloum & Schlenoff, 2004). In the present study, the amounts of protein adsorbed are comparable to a limited adsorption. From the molecular sizes and weights of the proteins it is possible to calculate the adsorbed amount for monolayer coverage. Assuming that both BLG and BSA can be represented as an equivalent sphere in solution, with hydrodynamic radii of 2.93 (Baldini et al., 1999), and 3.7 nm (Carter & Ho, 1994), and that surface coverage is 60% of the available area, then monolayer adsorption for both BLG and BSA would give an adsorbed amount of ~130 ng $cm^{-2}$. For a furcellaran terminated multilayer at pH 5, the amount adsorbed is equivalent to the deposition of ~5 protein layers. As pH is increased towards neutrality the amount adsorbed decreases, in a similar way to that observed for the binding of human serum albumin to a polyglutamic acid terminated layer. For polyanion/protein

complexes, decreases in the ability of the polyanion to complex protein are also observed in this pH range (Hallberg & Dubin, 1998). It is proposed that in the current study, that the furcellaran terminated layer is relatively permeable to the globular proteins and allows their complexation.

## 4. Conclusions

The results showed that furcellaran can be used to fabricate multilayer structures with PLL by a layer-by-layer technique. These structures can bind the globular proteins, BSA and BLG, the pH dependence of the binding is comparable to the observed complexation behaviour of furcellaran with globular proteins in aqueous solution, with complexation occurring at pHs where both biopolymers carry an average net charge of the same sign.

## Acknowledgements

The authors thank the BBSRC core strategic grant for financial support; and the Ministry of Education and Research of Estonia and Archimedes Foundation for the award of Kristjan Jaak fellowship to K.L. (Contract Number 0.06-04/06).

## References

Baldini, G., Beretta, S., Chirico, G., Franz, H., Maccioni, E., Mariani, P., et al. (1999). Salt-induced association of beta-lactoglobulin by light and X-ray scattering. *Macromolecules, 32*, 6128–6138.

Burke, S. E., & Barrett, C. J. (2003). pH-responsive properties of multilayered poly(L-lysine)/hyaluronic acid surfaces. *Biomacromolecules, 4*, 1773–1783.

Cannan, R. K., Palmer, A. H., & Kibrick, A. C. (1942). The hydrogen ion dissociation curve of beta-lactoglobulin. *Journal of Biological Chemistry, 142*, 803–822.

Carter, D. C., & Ho, J. X. (1994). Structure of serum albumin. *Advances in Protein Chemistry, 45*, 153–203.

Caruso, F., Furlong, D. N., Ariga, K., Ichinose, I., & Kunitake, T. (1998). Characterization of poly electrolyte–protein multilayer films by atomic force microscopy, scanning electron microscopy, and Fourier transform infrared reflection-absorption spectroscopy. *Langmuir, 14*, 4559–4565.

Decher, G. (1997). Fuzzy nanoassemblies: Toward layered polymeric multicomposites. *Science, 277*, 1232–1237.

Dubas, S. T., & Schlenoff, J. B. (2001). Swelling and smoothing of polyelectrolyte multilayers by salt. *Langmuir, 17*, 7725–7727.

Elbert, D. L., Herbert, C. B., & Hubbell, J. A. (1999). Thin polymer layers formed by polyelectrolyte multilayer techniques on biological surfaces. *Langmuir, 15*, 5355–5362.

Gergely, C., Bahi, S., Szalontai, B., Flores, H., Schaaf, P., Voegel, J. C., et al. (2004). Human serum albumin self-assembly on weak polyelectrolyte multilayer films structurally modified by pH changes. *Langmuir, 20*, 5575–5582.

Glinel, K., Prevot, M., Krustev, R., Sukhorukov, G. B., Jonas, A. M., & Mohwald, H. (2004). Control of the water permeability of polyelectrolyte multilayers by deposition of charged paraffin particles. *Langmuir, 20*, 4898–4902.

Hallberg, R. K., & Dubin, P. L. (1998). Effect of pH on the binding of beta-lactoglobulin to sodium polystyrenesulfonate. *Journal of Physical Chemistry B, 102*, 8629–8633.

Hook, F. (1997). PhD thesis, Chalmers University of Technology, Gothenburg, Sweden.

Jackson, M., Haris, P. I., & Chapman, D. (1989). Conformational transitions in poly(L-lysine) – studies using Fourier transform infra-red spectroscopy. *Biochimica et Biophysica Acta, 998*, 75–79.

Jung, L. S., Campbell, C. T., Chinowsky, T. M., Mar, M. N., & Yee, S. S. (1998). Quantitative interpretation of the response of surface plasmon resonance sensors to adsorbed films. *Langmuir, 14*, 5636–5648.

Krzeminski, A., Marudova, M., Moffat, J., Noel, T. R., Parker, R., Wellner, N., et al. (2006). The formation of pectin/poly-L-lysine multilayers with pectins of varying degrees of esterification. *Biomacromolecules, 7*, 498–506.

Ladam, G., Gergely, C., Senger, B., Decher, G., Voegel, J. C., Schaaf, P., et al. (2000). Protein interactions with polyelectrolyte multilayers: Interactions between human serum albumin and polystyrene sulfonate/polyallylamine multilayers. *Biomacromolecules, 1*, 674–687.

Lahaye, M. (2001). Developments on gelling algal galactans, their structure and physico-chemistry. *Journal of Applied Phycology, 13*, 173–184.

Laos, K., Brownsey, G. J., & Ring, S. G. (2005). Interactions between furcelleran and the globular proteins bovine serum albumin and beta lactoglobulin. *Carbohydrate Polymers*.

Lavalle, P., Picart, C., Mutterer, J., Gergely, C., Reiss, H., Voegel, J. C., et al. (2004). Modeling the buildup of polyelectrolyte multilayer films having exponential growth. *Journal of Physical Chemistry B, 108*, 635–648.

Lavalle, P., Vivet, V., Jessel, N., Decher, G., Voegel, J. C., Mesini, P. J., et al. (2004). Direct evidence for vertical diffusion and exchange processes of polyanions and polycations in polyelectrolyte multilayer films. *Macromolecules, 37*, 1159–1162.

Marudova, M., Lang, S., Brownsey, G. J., & Ring, S. G. (2005). Pectin–chitosan multilayer formation. *Carbohydrate Research, 340*, 2144–2149.

Mattison, K. W., Dubin, P. L., & Brittain, I. J. (1998). Complex formation between bovine serum albumin and strong poly electrolytes: Effect of polymer charge density. *Journal of Physical Chemistry B, 102*, 3830–3836.

Michel, M., Vautier, D., Voegel, J. C., Schaaf, P., & Ball, V. (2004). Layer by layer serf-assembled polyelectrolyte multilayers with embedded phospholipid vesicles. *Langmuir, 20*, 4835–4839.

Pereira, L., Sousa, A., Coelho, H., Amado, A. M., & Ribeiro-Claro, P. J. A. (2003). Use of FTIR, FT-Raman and (13)GNMR spectroscopy for identification of some seaweed phycocolloids. *Biomolecular Engineering, 20*, 223–228.

Picart, C., Mutterer, J., Richert, L., Luo, Y., Prestwich, G. D., Schaaf, P., et al. (2002). Molecular basis for the explanation of the exponential growth of polyelectrolyte multilayers. *Proceedings of the National Academy of Sciences of the United States of America, 99*, 12531–12535.

Quinn, J. F., & Caruso, F. (2004). Facile tailoring of film morphology and release properties using layer-by-layer assembly of thermoresponsive materials. *Langmuir, 20*, 20–22.

Richert, L., Lavalle, P., Payan, E., Shu, X. Z., Prestwich, G. D., Stoltz, J. F., et al. (2004). Layer by layer buildup of polysaccharide films: Physical chemistry and cellular adhesion aspects. *Langmuir, 20*, 448–458.

Salloum, D. S., & Schlenoff, J. B. (2004). Protein adsorption modalities on polyelectrolyte multilayers. *Biomacromolecules, 5*, 1089–1096.

Sauerbrey, G. (1959). Use of a quartz crystal vibrator for weighing thin films on a microbalance. *Zeitschrift fur Physik, 155*, 206–222.

Schlenoff, J. B., Ly, H., & Li, M. (1998). Charge and mass balance in polyelectrolyte multilayers. *Journal of the American Chemical Society, 120*, 7626–7634.

Seyrek, E., Dubin, P. L., Tribet, C., & Gamble, E. A. (2003). Ionic strength dependence of protein–polyelectrolyte interactions. *Biomacromolecules, 4*, 273–282.

Shi, X. Y., & Caruso, F. (2001). Release behavior of thin-walled microcapsules composed of polyelectrolyte multilayers. *Langmuir, 17*, 2036–2042.

Shiratori, S. S., & Rubner, M. F. (2000). pH-dependent thickness behavior of sequentially adsorbed layers of weak polyelectrolytes. *Macromolecules, 33*, 4213–4219.

Sui, Z. J., Salloum, D., & Schlenoff, J. B. (2003). Effect of molecular weight on the construction of polyelectrolyte multilayers: Stripping versus sticking. *Langmuir, 19*, 2491–2495.

Sukhishvili, S. A., Dhinojwala, A., & Granick, S. (1999). How polyelectrolyte adsorption depends on history: A combined Fourier transform infrared spectroscopy in attenuated total reflection and surface forces study. *Langmuir, 15*, 8474–8482.

Sukhishvili, S. A., & Granick, S. (1999). Adsorption of human serum albumin: Dependence on molecular architecture of the oppositely charged surface. *Journal of Chemical Physics, 110*, 10153–10161.

Tanford, C., Swanson, S. A., & Shore, W. S. (1955). Hydrogen ion equilibria of bovine serum albumin. *Journal of the American Chemical Society, 11*, 6414–6421.

Truus, K., Vaher, M., Usov, A. I., Pehk, T., & Kollist, A. (1997). Gelling galactans from the algal community of Furcellaria lumbricalis and *Coccotylus truncatus* (the Baltic Sea, Estonia): A structure–property study. *International Journal of Biological Macromolecules, 21*, 89–96.

Voinova, M. V., Rodahl, M., Jonson, M., & Kasemo, B. (1999). Viscoelastic acoustic response of layered polymer films at fluid–solid interfaces: Continuum mechanics approach. *Physica Scripta, 59*, 391–396.

Volery, P., Besson, R., & Schaffer-Lequart, C. (2004). Characterization of commercial carrageenans by Fourier transform infrared spectroscopy using single-reflection attenuated total reflection. *Journal of Agricultural and Food Chemistry, 52*, 7457–7463.